

ACCELERATED CARBIDE SPHEROIDISATION AND REFINEMENT (ASR) OF THE C45 STEEL DURING CONTROLLED ROLLING

POSPEŠENA SFEROIDIZACIJA IN UDROBNJENJE KARBIDOV (ASR) PRI KONTROLIRANEM VALJANJU JEKLA C45

Daniela Hauserova, Jaromir Dlouhy, Zbysek Novy

COMTES FHT, Prumyslova 995, 334 41 Dobruška, Czech Republic
daniela.hauserova@comtesfht.cz

Prejem rokopisa – received: 2013-10-14; sprejem za objavo – accepted for publication: 2013-11-06

Current industry trends include the search for cost- and energy-saving procedures and technologies. A new process has been discovered recently, which allows a significant refinement of ferrite grains and a carbide spheroidisation in a shorter time than in the case of conventional heat-treatment techniques. During this newly-developed ASR-based (accelerated spheroidisation and refinement) plastic deformation an accelerated spheroidisation and a refinement due to the heat treatment in the vicinity of the A_1 temperature occur.

Controlled rolling enables a production of the materials with a fine microstructure and better mechanical properties than conventional production processes. Accelerated carbide spheroidisation and refinement (ASR) is aimed to produce steel workpieces with a microstructure consisting of a fine-grained ferrite matrix and globular carbide particles. In carbon steels, this microstructure has higher yield strength and toughness than the conventional ferritic-pearlitic microstructure.

The presented paper describes the effect of the ASR process on the C45 steel. The pearlite morphology was influenced by forming it at the temperatures around critical temperature A_1 and an accelerated carbide-particle spheroidisation was achieved. The deformation increases the dislocation density and enhances the diffusion rate. Cementite globules form rapidly, within seconds or minutes at the most.

Keywords: accelerated spheroidisation, refinement, rolling, C45 steel

Sedanje usmeritve industrije vključujejo tudi iskanje stroškovno in energijsko ugodnejših postopkov in tehnologij. Razvit je bil nov postopek, ki omogoča znatno udrobnjenje zrn ferita in sferoidizacijo karbidov v krajšem času v primerjavi s konvencionalnimi tehnikami toplotne obdelave. Pri tej novo razviti plastični deformaciji, na kateri temelji ASR (pospešena sferoidizacija in udrobnjenje), se pri plastični deformaciji pojavi pospešena sferoidizacija in udrobnjenje med toplotno obdelavo v bližini temperature A_1 .

Kontrolirano valjanje omogoča izdelavo materialov z drobno mikrostrukturo in z boljšimi mehanskimi lastnostmi kot pri navadnih proizvodnih procesih. Namen pospešene sferoidizacije karbidov in udrobnjenja zrn (ASR) je izdelava jekla z mikrostrukturo iz drobnih zrn ferita in globularnih karbidnih zrn. Pri ogljikovih jeklih ima ta mikrostruktura višjo mejo tečenja in večjo žilavost kot navadna feritno-perlitna mikrostruktura.

Članek opisuje učinek ASR-procesa na jeklo C45. Na morfologijo perlita se vpliva s preoblikovanjem pri temperaturah okrog kritične temperature A_1 , in s tem je dosežena sferoidizacija karbidnih delcev. Deformacija povečuje gostoto dislokacij in poveča hitrost difuzije. Globularni cementit največkrat nastane v nekaj sekundah ali minutah.

Ključne besede: pospešena sferoidizacija, udrobnjenje, valjanje, jeklo C45

1 INTRODUCTION

The current processes leading to a carbide-particle spheroidisation rely on diffusion of carbon in a workpiece heated to a temperature close to or slightly below A_{c1} .¹ Diffusion-based processes of this type are usually time-consuming and the times of up to tens of hours² make this type of annealing a very expensive heat-treatment process. During annealing, softening processes occur in the microstructure and, in some cases, a recovery and a recrystallization also take place.³ The strength and hardness of the steel workpiece decline, whereas its ductility and plastic-deformation capability are increased. The newly-designed and patented thermo-mechanical process brings a several-fold reduction in the processing time and cost.^{4,5}

The present paper describes an investigation of the influence of the plastic-deformation intensity and strain

applied at various stages of transformation on the steel microstructure and mechanical properties. A significant acceleration of the process is due to the steel heating at a temperature just below transformation temperature A_{c1} and the plastic strain.⁶

2 EXPERIMENTAL WORK

2.1 Material and thermomechanical treatment

The experimental work was performed using the carbon steel C45 with the chemical composition listed in **Table 1**. The initial microstructure consisted of ferrite and lamellar pearlite with pronounced banding along the bar axis (**Figure 1**). The hardness of the as-received material was 180 HV, the 0.2 proof stress was 345 MPa, the ultimate tensile strength was 629 MPa, the elongation was $A_5 = 29 \%$ and the impact toughness was $KCV = 29 \text{ J/cm}^2$.

Table 1: Chemical composition of the C45 steel (mass fractions, w/%)

Tabela 1: Kemijska sestava jekla C45 (masni deleži, w/%)

| | | | | | | | | | |
|------|------|------|-------|-------|------|------|------|------|------|
| C | Si | Mn | S | P | Cr | Ni | Cu | Mo | W |
| 0.42 | 0.24 | 0.69 | 0.019 | 0.016 | 0.12 | 0.16 | 0.12 | 0.02 | 0.01 |

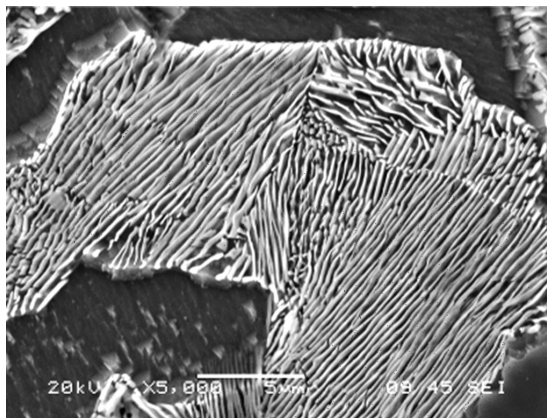


Figure 1: SEM micrograph of the initial state

Slika 1: SEM-posnetek začetne mikrostrukture

The thermomechanical treatment was carried out in a universal rolling mill that can be configured as either a four-high rolling mill or a two-high mill. The two-high configuration is used for hot rolling. The working roll diameter is 550 mm. The maximum width of the rolled plate is 400 mm and the thickness may range from 100 mm to 5 mm. The maximum rolling speed is 1.5 m/s. During rolling the induction heating system, situated on both sides of the rolling mill, can be used and a water-spray facility for quenching is provided on the mill. The rolling mill also includes hydraulic shears. The initial dimensions of the specimens for thermomechanical treatment were 330 mm × 50 mm × 30 mm.

Thermomechanical-treatment schedules (Table 2) were proposed for investigating the impact of the strain magnitude and the strains applied at various stages of the pearlitic transformation on the microstructure and mechanical properties. The main focus was the degree of carbide spheroidisation and ferrite-grain refinement.

Austenitizing at 850 °C was followed by a thickness reduction with the isothermal strain of $\varphi = 0.4$. Before the second and third deformations, the specimens were air cooled. The second and third deformation steps were applied at various stages of the austenite-to-pearlite

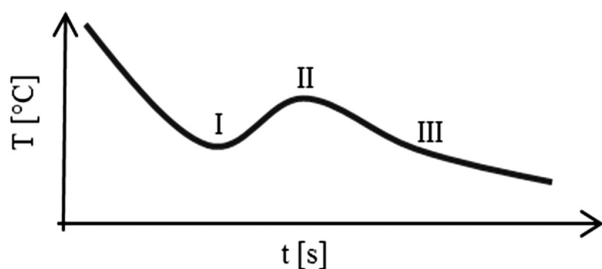


Figure 2: Transformation stages during deformation

Slika 2: Faze transformacije pri deformaciji

transformation (I, II, III – Figure 2). The strain magnitudes applied at these lower temperatures and at various stages of the pearlitic transformation were 0.5 (one pass) or 1 (two passes). When two passes were used, they immediately followed each other and took place at a virtually equal temperature. The temperature at point I was approximately 675 °C. At point II, it was 685 °C and at point III it was 675 °C. In all the cases, the deformation speed was 1.5 m/s. After the last pass, the specimens were either air cooled or quenched in water. The quenching immediately followed the last pass to allow a later determination of the austenite content.

3 RESULTS AND DISCUSSION

3.1 Metallographic observation

Specimens 1w, 2w, 3w were processed using the schedules with a deformation at 850 °C applied at various stages of the transformation (I, II, III) and quenched in water. The metallographic examination clearly revealed varying amounts of martensite in the microstructure. In the course of the last deformation, the expected austenite amounts in the specimens in schedules 1w, 2w and 3w were approximately 50 %, 25 % and 10 % max., respectively. These fractions correspond

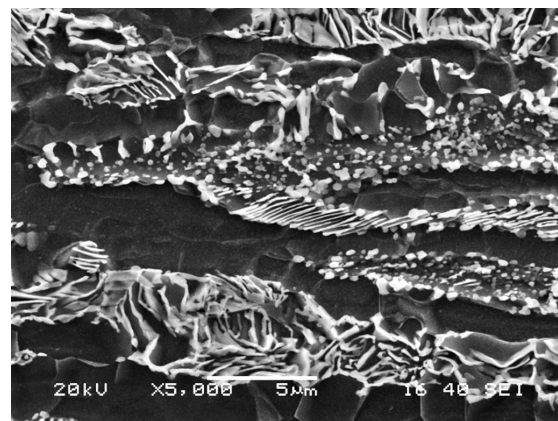


Figure 3: SEM micrograph of the 4a specimen

Slika 3: SEM-posnetek mikrostrukture vzorca 4a

Table 2: List of schedules

Tabela 2: Seznam poteka preizkusov

| Schedule | Temperature of first deformation $\varphi = 0.4$ | Temperature of second deformation $\varphi = 0.5$ | Temperature of third deformation $\varphi = 0.5$ | Cooling |
|----------|--|---|--|---------|
| 1a | 850 °C | I | - | Air |
| 1w | 850 °C | I | - | Water |
| 2a | 850 °C | II | - | Air |
| 2w | 850 °C | II | - | Water |
| 3a | 850 °C | III | - | Air |
| 3w | 850 °C | III | - | Water |
| 4a | 850 °C | I | I | Air |
| 4w | 850 °C | I | I | Water |
| 5a | 850 °C | II | II | Air |
| 5w | 850 °C | II | II | Water |
| 6a | 850 °C | III | III | Air |
| 6w | 850 °C | III | III | Water |

to the fractions of lamellar pearlite in the air-cooled specimens (1a, 2a, 3a). The lamellar pearlite exhibits no sign of spheroidisation or lamellae fragmentation and it is assumed that the pearlite formed after the deformation. However, in the pearlite already present in the microstructure during the last deformation, the lamellae were transformed into elongated particles or, less frequently, to globules and only a small fraction of the initial pearlite lamellae spheroidised completely.

The 4a, 5a and 6a schedules comprised a deformation at 850 °C, consisting of two deformation steps at various stages of transformation, and the final air cooling. The specimens contained two pearlite morphologies, as in the 1a, 2a and 3a specimens, with parts of lamellar pearlite and, by regions, with globules and rod-like cementite particles. The fraction of lamellar pearlite decreases from the 4a to the 6a schedule (Figures 3 and 4), i.e., with the progress of transformation of the austenite present during the plastic deformation. The amount of austenite was found by mapping the martensite fraction in water-quenched specimens 4w, 5w and 6w, with the decreasing martensite proportion in this order.

The mechanical deformation of austenite at transformation stages I or II (Figure 2) caused it to transform to lamellar pearlite, as in the transformation of the austenite unaffected by deformation. The deformation of lamellar pearlite with the strain magnitude $\varphi = 0.5$ at stages I, II or III led to a fragmentation of the lamellae and to a formation of predominantly elongated cementite particles. Strain magnitude 1 (i.e., two passes with the strains of 0.5) caused a partial spheroidisation of pearlite lamellae at all the stages of the pearlitic transformation, producing cementite in the form of globules and rod-like particles.

3.2 Ferrite Grains

The characteristics of the ferrite grains in the microstructure depend strongly on the transformation stage (I, II or III), at which deformation was applied (Figure 2).

The strain of 0.5 applied at stage I led to a 90 % recrystallization of ferrite. The resulting grain size was less than 8 μm (Figure 5). The strain of 0.5 applied at

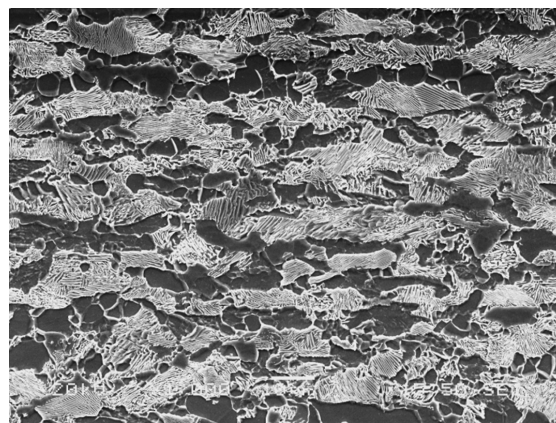


Figure 5: SEM micrograph of the 1a specimen

Slika 5: SEM-posnetek mikrostrukture vzorca 1a

stages II and III caused a recrystallization of only a small fraction of ferrite grains. Approximately 80 % of the ferrite grains exhibited a deformation substructure with elongated grains and deformation-induced subgrains (Figure 6). The size of the elongated ferrite grains was approximately 20 μm .

In the case of the strain of magnitude 1, the differences between the ferrite grains after the schedules involving the deformation at stages I and III were smaller. The larger strain caused a recrystallization of approximately 50 % of the ferrite grains even after the deformation applied at stage III (Figures 4 and 7). Upon schedules 4a, 5a and 6a, the size of the recrystallized grains was 4 μm . Scarcely recrystallized grains with the size of approximately 10 μm were also observed. With an EBSD analysis the grain size and the volume fractions of deformed and recrystallized grains could be assessed.

3.3 Mechanical properties

Tensile tests were performed on the flat specimens with the dimensions of 35 mm \times 6 mm \times 4 mm. The V-notch impact-toughness test-specimen size was 3 mm \times 4 mm with the notch depth of 1 mm. The HV10 hardness was measured as well.

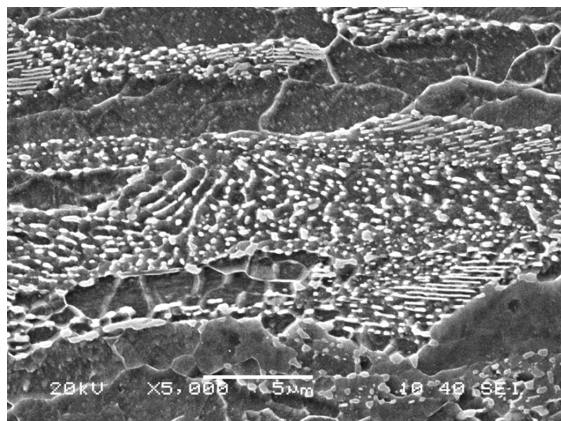


Figure 4: SEM micrograph of the 6a specimen

Slika 4: SEM-posnetek mikrostrukture vzorca 6a

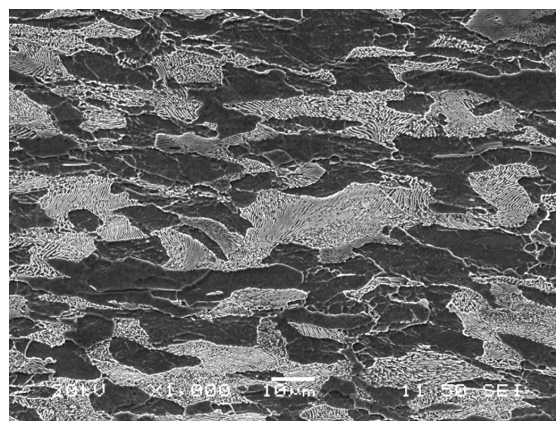


Figure 6: SEM micrograph of the 3a specimen

Slika 6: SEM-posnetek mikrostrukture vzorca 3a

Different proof stresses and ultimate strengths were measured for three specimens upon these schedules (**Table 3**). One of the three specimens showed approximately 50 MPa higher proof stress and ultimate tensile strength than the others. The figures listed in **Table 3** are the average values of three tests.

Table 3: Mechanical properties

Tabela 3: Mehanske lastnosti

| Schedule | PS/ MPa | UTS/ MPa | A ₅ / % | KCV/ (J cm ⁻²) | HV 10 |
|--------------------------|------------|-------------|-----------------------|-------------------------------|-------|
| Initial condition | 345 | 629 | 29 | 29 | 180 |
| 1a | 489 | 702 | 26 | 38 | 204 |
| 2a | 511 | 710 | 25 | 36 | 213 |
| 3a | 542* | 688* | 21 | 35 | 201 |
| 4a | 547 | 709 | 28 | 36 | 212 |
| 5a | 550 | 708 | 27 | 35 | 210 |
| 6a | 534* | 668* | 25 | 35 | 199 |

Different properties will be the subject of a further investigation. All the thermomechanical treatment schedules led to higher proof stress, ultimate tensile strength, hardness and impact toughness (**Table 3**). The final elongation was slightly lower than, or equal to, the initial elongation. Upon the schedules with smaller strain magnitudes (1a, 2a and 3a) the following trends were observed for the specimens: If deformation was applied at an early stage of the pearlitic transformation [I], the resulting proof stress was the lowest of those measured. When deformation was applied at a later stage of the transformation [III], the resulting proof stress was higher. In the specimens under the schedules with higher strains (4a, 5a, 6a), this trend was not observed and their strengths were virtually equal. The schedules with the higher strains applied at the same transformation stage as in the other schedules lead to a higher proof stress. This observation does not apply to specimen 6a, as the strength levels achieved are very similar (**Table 3**). In terms of proof stress, less strain is sufficient ($\varphi = 0.5$), provided that it is applied at the final stage of the pearlitic transformation.

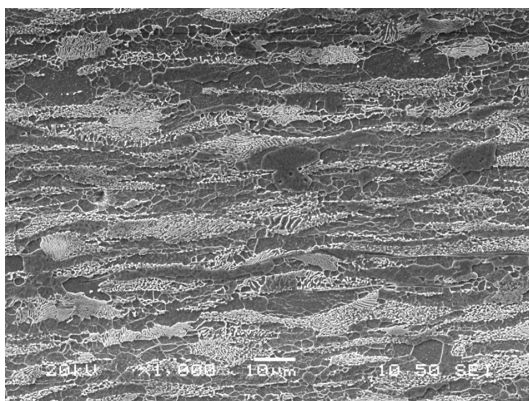


Figure 7: SEM micrograph of the 6a specimen
Slika 7: SEM-posnetek mikrostrukture vzorca 6a

4 CONCLUSION

The purpose of the investigation was to improve the mechanical properties, promote the carbide spheroidisation and refine the ferrite grains in the medium-carbon C45 steel using controlled rolling. The final deformation was applied in the intercritical range at various stages of the transformation of austenite into ferrite and carbide particles. In the specimens quenched in water after the final deformation, no carbide spheroidisation or fragmentation was observed. On the contrary, in the specimens cooled in air spheroidised carbides were observed. A higher proportion of spheroidised particles was found in the specimens after a larger final deformation with $\varphi = 1$. The fraction of spheroidised carbides increased with the applied strain magnitude at the advanced stages of transformation. The microstructure showed that after the deformation applied at the final stages of transformation, recrystallisation also took place in the ferrite grains. The proof stress and ultimate tensile strength of the processed material were higher by 200 MPa and almost 100 MPa, respectively, than the corresponding characteristics of the feedstock. The elongation levels were identical, whereas the toughness of the final material was slightly higher than that of the feedstock. The experimental rolling, thus, improved the mechanical properties, facilitated a partial spheroidisation of the carbides and required less time in comparison with the conventional carbide-spheroidising methods.

Acknowledgment

The results were achieved within the project Thermo-chemical treatment of steels using fluidised bed with thermoactive micropowders no. LF13032 co-funded by the Ministry of Education, Youth and Sports of the Czech Republic.

5 REFERENCES

- ¹ S. Ghosh, Rate-controlling parameters in the coarsening kinetics of cementite in Fe-0.6C steels during tempering, *Scripta Materialia*, 63 (2010) 3, 273–276
- ² K. G. Ata, S. A. Meisam, Spheroidizing Kinetics and Optimization of Heat Treatment Parameters in CK60Steel Using Taguchi Robust Design, *Journal of Iron and Steel Research*, 17 (2010) 4, 45–52
- ³ W. J. Nam, C. M. Bae, Coarsening Behavior of Cementite Particles at a Subcritical temperature in a medium Carbon Steel, *Scripta Materialia*, 41 (1999) 3, 313–318
- ⁴ B. Masek, H. Jirkova, L. Kucerova, Rapid Spheroidization and Grain Refinement Caused by Thermomechanical Treatment for Plain Structural Steel, *Materials Science Forum*, 706–709 (2012), 2770–2775
- ⁵ H. Jirkova, D. Hauserova, L. Kucerova, B. Masek, Energy and Time Saving Low Temperature Thermomechanical Treatment of Low Carbon Plain Steel, *Mater. Tehnol.*, 47 (2013) 3, 335–339
- ⁶ S. L. Zhang, X. J. Sun., H. Dong, Effect of deformation on the evolution of spheroidization for the ultra high carbon steel, *Materials Science and Engineering*, 432 (2006) 1–2, 324–332